Exp Astron (2015) 39:281–302
DOI 10.1007/s10686-015-9448-z

ORIGINAL ARTICLE

Status of the eLISA on table (LOT) electro-optical simulator for space based, long arms interferometers

Pierre Grüning · Hubert Halloin · Pierre Prat · Sylvain Baron · Julien Brossard · Christelle Buy · Antoine Petiteau · Gerhard Heinzel · Iouri Bykov

Received: 18 April 2014 / Accepted: 22 February 2015 / Published online: 15 March 2015

Abstract We report on the progress in the realization of an electronic / optical simulator for space based, long arm interferometry and its application to the eLISA mission. The goal of this work is to generate realistic optics and electronics signals, especially simulating realistic propagation delays. The first measurements to characterize the simulator are also presented. With the present configuration, noise reduction factors of 5×10^7 for optical beat notes and 10^9 for RF beat notes have been achieved using the Time Delay Interferometry algorithm. The principle of the experiment has been validated and further work is ongoing to identify the residual noise sources and optimize the apparatus.

Keywords Interferometry · eLISA · Gravitational waves · Experimental validation · Time delay interferometry

1 Introduction

The evolved Laser Interferometer Space Antenna (eLISA) is a space-based project aiming at detecting gravitational waves in the frequency range 0.1 mHz to 1 Hz. eLISA consists of 3 spacecrafts (S/C) in a nearly-equilateral configuration, constantly following free-falling masses located at their center and orbiting around the sun [2].

P. Grüning (✉) · H. Halloin · P. Prat · S. Baron · J. Brossard · C. Buy · A. Petiteau
APC, AstroParticule et Cosmologie, Université Paris Diderot, CNRS/IN2P3, CEA/Irfu, Observatoire de Paris, Sorbonne Paris Cité, 10, rue Alice Domon et Léonie Duquet, 75205 Paris Cedex 13, France
e-mail: pierre.gruning@apc.univ-paris7.fr

G. Heinzel · I. Bykov
Max-Planck-Institut für Gravitationsphysik (Albert-Einstein-Institut), Callinstraße 38, 30167 Hannover, Germany

eLISA is the straw man concept proposed as an ESA L-class mission to fulfill the scientific objectives of 'The Gravitational Universe' proposed science theme. This theme has recently been selected by ESA for a launch in 2034. The eLISA concept follows the extensively studied LISA project [4, 11] and evolved out of the NGO study [12].

In the eLISA concept, a 'mother' spacecraft is located at the vertex of a V-shaped configuration, with two 'daughter' spacecraft at the end of the two arms. Laser beams are propagating along the arms, effectively forming a Michelson-type interferometer with 10^6 km arm lengths. The spacecraft follows independent heliocentric orbits and forms a nearly equilateral triangle in a plane that is inclined by 60° against the ecliptic (see Fig. 1). Furthermore, Fig. 1 shows also the expected noise curve and associated sensitivity curve convolved with the eLISA response to the gravitational waves. More details on the sensitivity computation and science objectives of eLISA can be found in [2, 3, 12] and references therein.

Four interferometric measurements are used to precisely monitor the distances between the inertial masses and, hence, to detect the tiny variations in their distance due to the pass of a gravitational wave, two on the mother S/C which contains two free-falling masses and one on each daughter S/C. The goal of eLISA is to detect gravitational deformation as small as $\Delta L/L \approx 10^{-20}/\sqrt{\text{Hz}}$ (i.e 10 pm per million km) in a frequency band of 10^{-4} Hz to 1 Hz.

This expected performance of eLISA relies on two main technical challenges: the ability for the spacecraft to precisely follow the free-flying masses and the outstanding precision of the phase shift measurement between the spacecrafts.

To meet these requirements, the payload of eLISA consists of four identical units, two on the mother spacecraft and one on each daughter spacecraft. Each unit contains a Gravitational Reference Sensor (GRS) with an embedded free-falling test mass that acts both as the end point of the optical length measurement and as a geodesic reference test particle. A telescope with 20 cm diameter transmits light from a 2W laser at 1064 nm along the arm and also receives a small fraction of the light sent from the far spacecraft. The required laser beat signals are formed on an optical bench in between the telescope and the GRS (see Fig. 2).

Unlike ground-based detectors, a major feature of space-based interferometry between inertial references is the length mismatch of the arms and its time

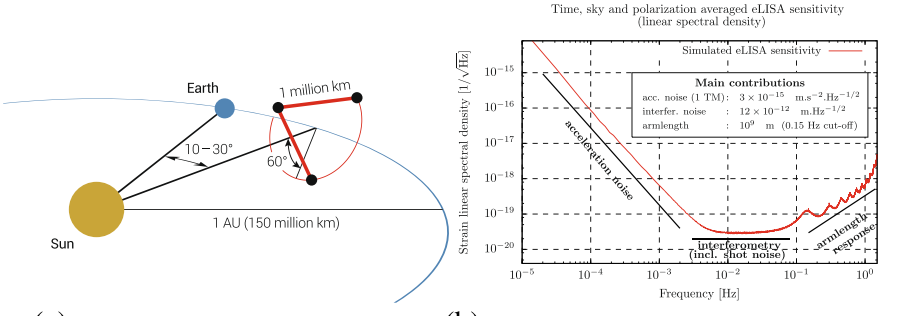

(a) The V-shaped constellation of eLISA. [2] (b) eLISA noise spectrum (averaged strain sensitivity).

Fig. 1 eLISA configuration and sensitivity curve

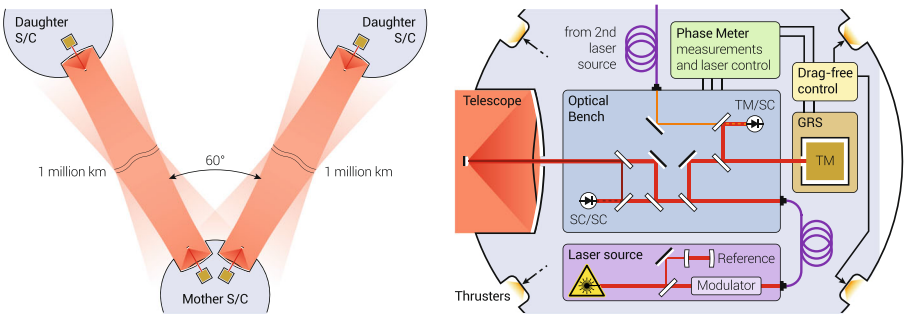

(a) Scheme of the eLISA interferometer. (b) The eLISA payload.

Fig. 2 Measurement principle of eLISA [2]

dependance. Actually, the arm length difference will be up to 3×10^4 km with relative velocities up to 7 m/s. As a consequence of the length mismatch, the different propagation delays along the two arms have to be taken into account in the post-processing algorithm to avoid the coupling of the laser frequency noise with the science signal. This algorithm is known as "Time Delay Interferometry" (TDI) [5, 6, 20, 21, 30, 31, 34, 35]. With a knowledge of the arm lengths at about 1 m accuracy, the laser frequency needs to be 'pre-stabilized' at a level of about $10^{-12}/\sqrt{\text{Hz}}$, using a ultra-stable Fabry-Perot cavity [29].

Another method, called arm-locking has been suggested to further decrease the laser frequency noise. The principles are described in [14, 22, 24, 27, 28, 37].

The measurement of the inter-spacecraft distance is done using a low frequency modulation of the laser frequency, transmitting and correlating pseudo-random codes. Another modulation (at about 1 GHz) is also required to transfer the noise of the on-board clocks and compensate for their effect on the analog to digital converters (ADC) timestamping [7, 8, 10, 13, 17, 23, 25, 26]. These beat notes carrying the 'science' as well as the ranging and clock synchronization signals, need to be measured at the level of the μcycle/$\sqrt{\text{Hz}}$ to reach the required eLISA sensitivity, while following the frequency drifts between 5 and 25 MHz, due to the relative motion of the S/C.

Hence, the capability of eLISA to measure very small displacements relies (among other things) on accurate processing algorithms (TDI), precise feedback loops (arm-locking) and very low noise, extremely high performance instruments (phasemeters). Software can simulate the Doppler effects, the propagation delays, reconstruction algorithms, etc (see e.g. [19]). Nevertheless, the development of hardware simulations are desirable, in order to characterize the detection devices, validate the numerical models and study the influence of the hardware on the detection algorithms. This is the purpose of the eLISA On Table (LOT) experiment developed at the APC laboratory and described in the next sections.

Hardware simulators for eLISA have already been developed by other teams in the project. Two approaches have been implemented so far: with realistic, electronically delayed, phase noises [15, 16] and optical, short arms experiments [36]. This paper describes an experimental setup allowing the simulation of optical links with

the appropriate noise delays and Doppler shifts. The LOT experiment can reproduce most of the features of the eLISA interferometry and the expected noise. It will also be possible to inject user-defined noise functions and accelerate the simulation to complete months of data simulation within days.

2 Experimental setup of eLISA

The goals of the LOT experiment is to be able to simulate optical beat notes, as representative as possible of the signals that will be recorded by eLISA. The experimental setup should also be kept very flexible to allow different configurations and the use of hardware prototypes, so that it could be adapted to new technologies or algorithms developed for eLISA.

Beyond the model of eLISA, the main challenge of such an experiment is to properly simulate delayed optical noise, while keeping the setup extremely stable on time scales of tens of seconds. The experimental setup presented here mainly focuses on the demonstration of the simulation principles and first results. The reduction of the interferometer intrinsic noises and complete development of eLISA functionalities will be addressed in the future.

2.1 eLISA model

The eLISA mission is composed of two arms, each of them linking one free-falling mass of the 'mother' spacecraft to the free-falling mass of each 'daughter' spacecraft. In practice, the variations of the arm length are computed from three interferometric measurements on each link: test mass to optical bench on the mother S/C, 'mother' optical bench to 'daughter' optical bench, optical bench to test mass on the daughter S/C. The sum of these 3 measurements cancels out the movement of the S/C w.r.t the test masses. The principle and different measurements of the eLISA interferometry is represented on Fig. 3.

eLISA consists of four (almost) identical payloads: two on the mother S/C, one on each daughter S/C. Each payload consists of one test mass, one laser source and one optical bench (plus the control electronics, such as the phasemeter, the charge management unit, the housekeeping data unit, etc, which are not represented on Fig. 3). The two daughter S/C act like "mirrors", each one containing a laser which is phase locked on the incoming laser from the mother S/C, this is the transponder mode. The three S/C are labelled 1, 2 and 3: 1 refers to the mother S/C and the others to the daughters. Following conventions inherited from the previous LISA project (which had three identical S/C), devices and 'information' propagating clockwise are labelled with 1, 2 and 3, whereas they are labelled 1', 2' and 3' when propagating counter-clockwise.

On the mother optical bench 1, three interferometric measurements are performed, giving the relative optical phase between:

– the local laser (Laser 1) and the incoming signal from S/C 2 (and optical bench 2'), i.e. optical bench 1 to distant S/C: $s_{OS;1}(t)$

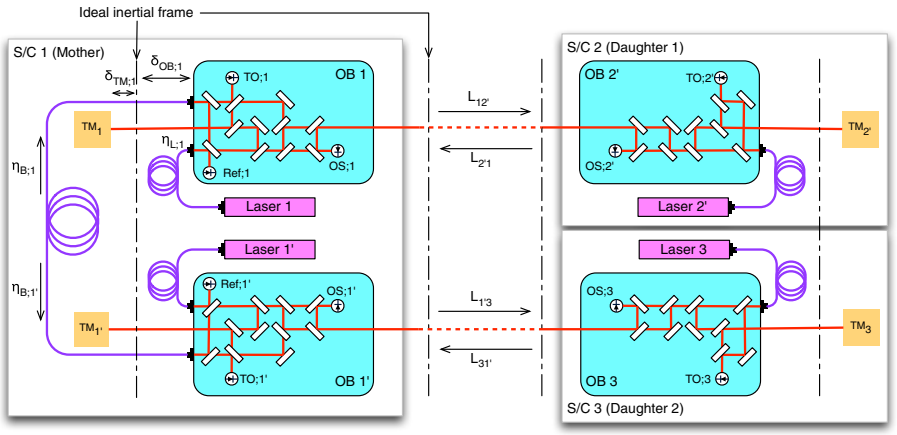

Fig. 3 Scheme of the interferometric measurements on the two arms of eLISA. See text for the explanations of the notations

- the adjacent laser (Laser 1') and the local laser (Laser 1) after reflection on the test mass 1 (TM_1), i.e. test mass to optical bench signal: $s_{TO;1}(t)$
- the local laser and the adjacent laser, i.e. reference signal: $s_{Ref;1}$

The second optical bench on the mother S/C is strictly identical. A 'back-link' fiber transfers the light from bench 1 to bench 1'(and vice versa). The optical benches on the daughter S/C are also identical except that there is only one optical bench (and one laser) per satellite, hence no reference beat note.

For the calculation, we will define the different positions noise w.r.t an ideal inertial frame, at the position of the S/C. With the notations of the figure, the different signals (phases) recorded on the optical bench can be expressed as:

$$s_{OS;1} = \phi_{R;2'1} - \delta_{OB;1} - \eta_{L;1} + o_{OS;1} \tag{1a}$$

$$s_{TO;1} = \eta_{L;1} + 2 \times (\delta_{OB;1} + \delta_{TM;1}) - \eta_{L;1'} - \eta_{B;1} + o_{TO;1} \tag{1b}$$

$$s_{Ref;1} = \eta_{L;1} - \eta_{L;1'} - \eta_{B;1} + o_{Ref;1} \tag{1c}$$

$$\phi_{S;12'} = \eta_{L;1} - \delta_{OB;1} + o_{S;12'}, \tag{1d}$$

where:

- $\phi_{R;2'1}$ is the phase of the laser beam received from optical bench 2'
- $\delta_{OB;1}$ is the phase noise due to the movement of the S/C 1 w.r.t the inertial frame mainly due to thruster noise
- $\eta_{L;1}$ is the phase noise of the laser source 1 and $\eta_{L;1'}$ for the adjacent laser source
- δ_{TM_1} is the phase variation induced by the movement of the test mass due to the residual acceleration noise
- $\eta_{B;1}$ is the additional phase noise in the back link fiber from bench 1' to 1
- $\phi_{S;12'}$ is the phase of the laser beam sent to optical bench 2' (w.r.t the inertial frame)

– $o_{xx;1}$ takes into account any local additional noise such as the optical bench phase noise

The same equations stand for the second optical bench of the mother S/C by replacing 1 with 1', 2 with 3' and 2' with 3. Similarly for optical bench 2', but with only one laser source:

$$s_{OS;2'} = \phi_{R;12'} - \delta_{OB;2'} - \eta_{L;2'} + o_{OS;2'} \tag{2a}$$
$$s_{TS;2'} = 2 \times (\delta_{OB;2'} + \delta_{TM;2'}) + o_{TS;2'} \tag{2b}$$
$$\phi_{S;2'1} = \eta_{L;2'} - \delta_{OB;2'} + o_{S;2'1} \tag{2c}$$

Moreover, the propagation along the arms between spacecrafts leads to:

$$\begin{aligned}\phi_{R;2'1} &= D_{2'1}\phi_{S;2'1} + g_{w;2'1} \\ &= D_{2'1}\eta_{L;2'} - D_{2'1}\delta_{OB;2'} + D_{2'1}o_{S;2'1} + g_{w;2'1},\end{aligned} \tag{3}$$

with similar equations for $\phi_{R;31'}$, $\phi_{R;12'}$ and $\phi_{R;1'3}$.

– D_{ij} is a delay operator: $D_{ij}\phi(t) = \phi(t - L_{ij})$ (L_{ij} being the light time from payload i to j, about 3.3 s)
– $g_{w;ij}$ is the perturbation due to a gravitational wave.

In eLISA, because of the relative motions of the S/C, $L_{ij} \neq L_{ji}$ (Sagnac effect) and $D_{ij}D_{kl}\phi \neq D_{kl}D_{ij}\phi$ (time evolving delays).

2.2 Time delay interferometry

Combining these measurements gives an equivalent measure of the phase of the test mass position w.r.t the incoming beam, corrected from the movement of the bench (w.r.t the test mass). Also, the LOT will be able to simulate the noise resulting from the fiber link from bench 1 to 1'(and vice-versa) using a second local arm in the future. The detailed steps to combine and simplify the equations using perfect transponder assumptions are detailed in Appendix A. Equations (8) and (9) form the set of time-delayed interferometry.

Finally, the 'test-mass to test mass' (8) signals become:

$$s_{TT;1} = D_{2'1}D_{12'}\eta_{L;1} - \eta_{L;1} + D_{2'1}g_{w;12'} + g_{w;2'1} \tag{4a}$$
$$s_{TT;1'} = D_{31'}D_{1'3}\eta_{L;1} - \eta_{L;1} + D_{31'}g_{w;1'3} + g_{w;31'} \tag{4b}$$
$$s_{TT;2'} = 0 \tag{4c}$$
$$s_{TT;3} = 0 \tag{4d}$$

The dominant noise terms are, by many orders of magnitudes, the laser phase fluctuations. These noises are however transported from one S/C to another and appear as differences between the local laser and the distant, delayed one. Their contribution can be canceled by properly delaying and combining the $S_{TT;q}$ signals: this method is known as time delay interferometry (TDI) (see e.g. [30]). TDI however requires a precise knowledge of the light time between S/C (at the meter level over 10^6 km). Moreover, these equations assumed perfect clocks on each S/C, with no relative drifts nor jitter. Ranging and clock noise transfer can be performed by adding

auxiliary modulations on the laser links [10]. After TDI and clock noise corrections [17], the residual phase noise should be due to the test masses (residual acceleration noise at low frequency) and the optical noise (including shot noise and path length fluctuations on the optical benches).

The primary goal of the LOT experiment is to optically simulate the $S_{TT;q}$ signals and then apply the TDI algorithm on the recorded signals, but it can also be configured to simulate any of the $s_{XX,q}$ signal. The simplified, 'transponder' equations which require only two simulated data streams, have been used for the first experimental measurements performed on the LOT, with the additional constraint of a static constellation (i.e $D_{2'1}D_{12'}$ and $D_{31'}D_{1'3}$ are constant and commute) and no gravitational wave signal. In that case, the simplest TDI combination (X, first generation) leads to:

$$X_{1^{st}} = (1 - D_{31'}D_{1'3})s_{TT;1} - (1 - D_{2'1}D_{1'2})s_{TT;1'} \tag{5}$$

This combination synthesized an equivalent Michelson interferometer with equal arms.

3 Experimental setup of LOT

Overview The goal of the eLISA On Table (LOT) experiment is to take an experimental approach of the main subjects of the eLISA mission such as phase noise or TDI (time delay interferometry). It is innovative insofar as it includes both electronic and optical aspects of a hardware simulator in one experiment and allows to simulate optical beatnotes with appropriate phase delays. Furthermore, as it is entirely computer controlled, the implementation of realistic noises and delays can be done through the use of software simulating the mission, such as LISAcode [18]. The LOT is expected to be a very complete optical simulator representative of eLISA, offering the additional flexibility to define ad-hoc fluctuations in the frequency, amplitude or phase of the laser and propagation delays. The control electronics also allows to 'accelerate' the simulation, so that one year of data streams could be generated within a few days.

3.1 Description of the electronic interferometer and electric TDI tests

The LOT's electronic part is composed of all necessary devices for control and measurement but also of an electronic version of the LOT established by combining the signals sent to acousto-optical modulators (AOMs). These electronic LOT signals can thus be analyzed and compared to the optical one. The concept is illustrated on Fig. 4.

3.1.1 Control-command and readout

Signal generation The data streams for each channel (i.e. sent to the AOMs) are simulated (i.e. generated, delayed and interpolated), converted to digital commands and sent to a National Instrument (NI) PXIe 6537 communication board. The frames (being 264 bits long) are serially sent on some of the 32 output ports of the NI card.

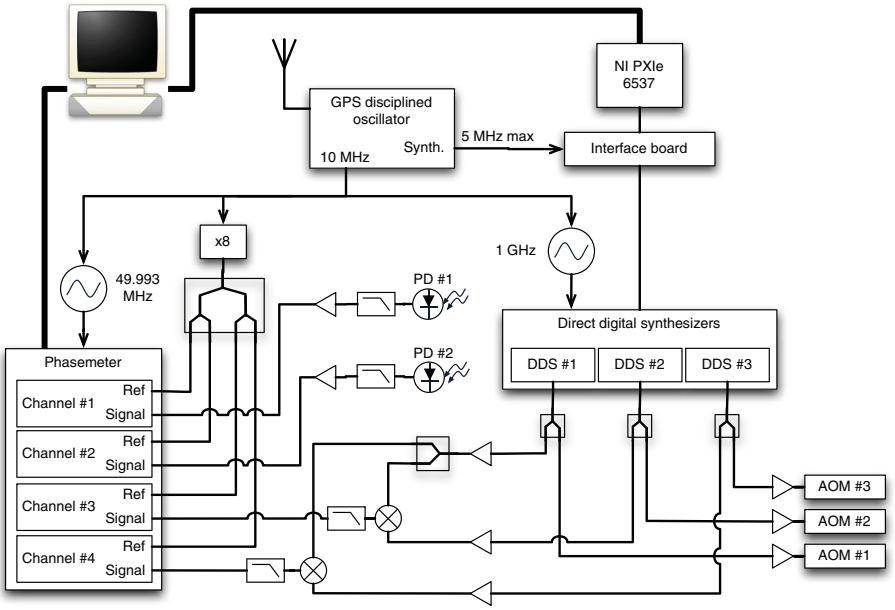

Fig. 4 Electronic scheme of the LOTNI PXIe: National Instrument chassis - DDS #i: Direct Digital Synthesizers channels - 49.993 MHz & 1 GHz: clock signals for the phasemeter and DDS - PD #i: photodiodes - AOM #i: Acousto-Optical Modulators receiving frequency modulation from DDS

The communication rate is controlled using a synthesized clock, up to 5 MHz, derived from the GPS disciplined oscillator. The communication card as well as the DDS can handle communication rates up to 50 MHz (i.e. a frames' rate of about 190 kHz), while it was set to 2 MHz in the present work (frames rate of 7.6 kHz).

Computer controlled DDS (Direct Digitial Synthesizer, model Agilent AD9912) are used to generate the analog signals from the data streams. The DDS are able to generate RF signals up to 400 MHz with an accuracy of 3.6 μHz and the possibility to adjust the phase of the signal with a precision of 0.38 mrad. The electronics clocks are derived from a 10 MHz high stability, GPS disciplined oscillator to reduce the differential jitter noise.

DDS channel #1 represents the local arm, channels #2 and #3 stand for the two distant arms. Channel #1 is mixed respectively with channel #2 and #3 in order to simulate the two beat signals of the transponder type configuration $s_{TT;1}$ and $s_{TT;1'}$ which can be injected into the first generation TDI algorithm (5). These two data streams are recorded by the phasemeter on channel #3 and #4.

Readout The phasemeter used in this study is a prototype developed by the Albert Einstein Institut in Hanover, Germany [1]. Within the phasemeters, the signals are digitized using an ADC (Analog to Digital Converter), running at the phasemeter reference clock (presently 49.993 MHz). The frequency measurements are then performed by monitoring the frequency of a digital phase locked loop. In order to compensate for the jitter noise of the input ADC, each channel is combined with a

80 MHz reference signal, produced from the octupled 10 MHz GPS frequency. This signal (folded at 20 MHz after sampling) is processed in the same way as the 'science' data and used to correct it. A residual noise lower than $1\mu\text{Hz}/\sqrt{\text{Hz}}$, for input frequencies between 2 and 20 MHz can be achieved. The output data are transmitted to the computer using a parallel port, at a rate of about 23.8 Hz. Both, the DDS and the phasemeter are controlled by a labview program with predefined mathematics models (computed by a separate C library for maximum efficiency) used to generate the RF frequencies and the simulated noise, including user-defined delays. These delays are held fixed in the present work, but will be representative of the eLISA orbits once the command program is combined with LISAcode [18, 19].

3.1.2 Electric TDI tests

Different configurations have been used to perform the first tests on the experimental setup described above. For all the measurements, the communication clock (synthesized from the GPS oscillator) was set to 2 MHz, meaning an update of the DDS data at a rate of 7.6 kHz. Given the theoretical DDS resolution of 3.6 μHz, such frequency and resolution lead to a quantization noise of about 3×10^{-8} Hz/$\sqrt{\text{Hz}}$.

Unless otherwise noted in the following descriptions, the carrier frequencies were set to 108 MHz ('local' arm), 112.5 MHz (Distant arm 1) and 112.7 MHz (Distant arm 2). These values lead to electronic beat notes around 4.5 and 4.7 MHz.

The frequency modulations of these carrier frequencies were simulated as gaussian white noises (sampling frequency of about 757.6 Hz) of amplitude 280 Hz/$\sqrt{\text{Hz}}$ (single sided amplitude spectral density), convolved with an 8^{th}-order low-pass filter (corner frequency of 10 Hz). This filter was needed to avoid extra interpolation noise close to the Nyquist frequency of the sampled noise. This simulated signal is delayed (according to the simulation parameters) and up-sampled to 7.6 kHz using a 15^{th} order Lagrange interpolation filter.

The delays were held constant, at 6.502081 s (arm 12) and 6.711826 s (arm 13). These values corresponds to typical round-trip delays on eLISA. These values are close to multiples of the phasemeter sampling period (155 and 160 respectively) to reduce interpolation noise. The reconstruction (interpolation) of the properly delayed phase measurement is done using a 31^{st} order Lagrange interpolation filter.

Four streams of data are recorded by the four-channel phasemeter (ordered from channel 1 to 4), here we present the electronic data streams $s_{e,1}$, $s_{e,1'}$ recorded on channel 3 and 4 (1 and 2 being used for the optical ones).

The amplitude spectral density (ASD) of the signals (raw or reconstructed) are computed on a logarithmic frequency axis using the algorithm described in [32, 33].

Intrinsic noise of the electric interferometer Three experiments have been conducted to estimate the intrinsic noise of the system and the analysis process.

First, the intrinsic noise level of the phasemeter has been estimated using a single RF source at 2.001 MHz, split on the 4 input channels of the phasemeter. The results are shown in Appendix B. However, the intrinsic phase noise of the phasemeter is well below the other noise sources of the LOT experiment and will not be a concern in the present work. For reference, the requirements for the interferometric measurement

(including shot noise, optical bench noise, electronics, etc.) are also plotted on Fig. 14.

On a second configuration, the 3 DDS were configured with no modulation, and carrier frequencies at 108.355 MHz ('local' arm), 112.572 MHz ('distant' arm 1) and 112.583 MHz ('distant' arm 2). The ASD of the resulting beat note, $s_{e,1}$ and the combination $s_{e,1}$ - $s_{e,1'}$ are represented on Fig. 5. The differential measurement is slightly lower than the raw signal, showing a correlation of the jitter between the different DDS. It could be due to a residual jitter noise between the 1 GHz synthesized signal (the DDS clock reference) and the RF reference signal at 80 MHz (from the octupled GPS frequency).

Applied to the present configuration, the 'Michelson' $X_{1^{st}}$ combination (see (5)) leads to:

$$X_{1^{st};x}(t) = s_{x,1}(t) - s_{x,1}(t-\tau_3) - \left[s_{x,1'}(t) - s_{x,1'}(t-\tau_2)\right], \tag{6}$$

where τ_3 is the simulated round-trip time between S/C 1 and 3 (6.711826 s) and τ_2 is the simulated round-trip time between S/C 1 and 2 (6.502081 s).

In the case of uncorrelated noise $s_{x,1}$ and $s_{x,1'}$ the amplitude spectral density of $X_{1^{st};x}$ is therefore given by:

$$\widetilde{X_{1^{st};x}}(\nu) = \sqrt{\widetilde{s_{x,1}}^2(\nu)\sin^2(\pi\tau_3\nu) + \widetilde{s_{x,1'}}^2(\nu)\sin^2(\pi\tau_2\nu)} \tag{7a}$$

$$= \widetilde{s_{x,1}}(\nu) \times \sqrt{1 - \cos\left(\pi\left(\tau_2+\tau_3\right)\nu\right)\cos(\pi(\tau_2-\tau_3)\nu)}, \tag{7b}$$

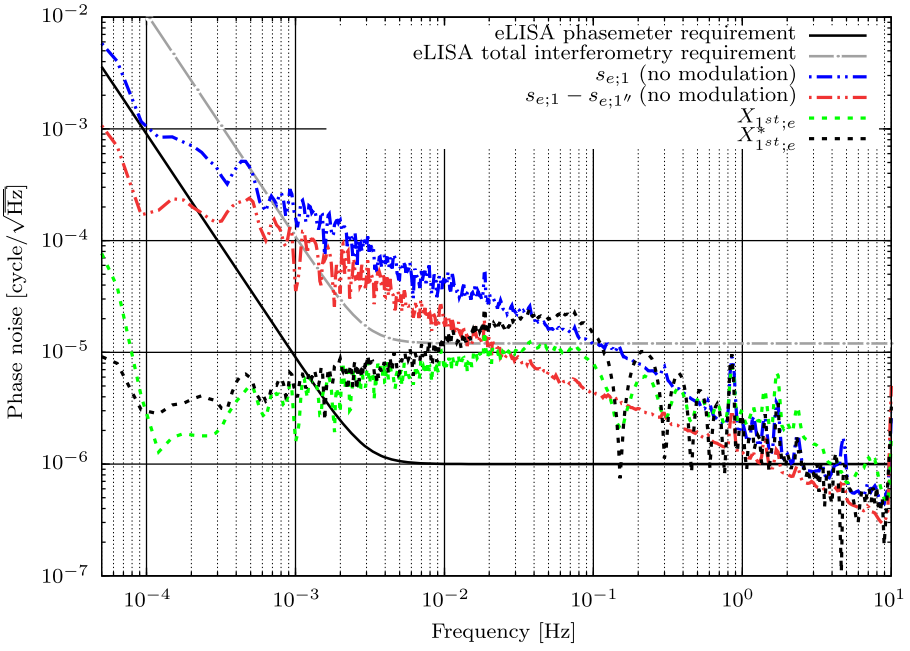

Fig. 5 Reference levels of noise in the electric LOT experiment: DDS and electronic noise

where (7b) assumes similar ASD for the $s_{x;q}$ signals ($\widetilde{s_{x,1}} = \widetilde{s_{x,1'}}$). With the same assumption and at low frequencies, we have $\widetilde{X_{1^{st};x}}(\nu) \approx \pi\sqrt{\tau_2^2+\tau_3^2}\times\nu\widetilde{s_{x,1}}(\nu)$: $X_{1^{st}}$ has a linear response function for $\nu \ll 2/(\tau_2+\tau_3)$.

This approximation (marked as $X^*_{1^{st}}$ in the plots) was tested on the recorded signal (with no modulation) and plotted on Fig. 5.

The results obtained after application of TDI and its theoretical model (transfer function) show identical behavior, especially the position of the nodes and the noise level. The observed discrepancies could be due to the correlation between the recorded signals. These noise levels are expected to be the noise floor of the present configuration of the electric LOT.

As a third test of the intrinsic noise of the experiment, the same frequency modulation (white frequency noise) has been applied on the two distant arms (see Fig. 6). This white noise (at a level of 560 Hz/$\sqrt{\text{Hz}}$ up to 1 Hz) is about twice the expected level of frequency noise of the stabilized laser source. The data were processed as described above, applying TDI with the same delay (6.502081 s) on the two arms.

Figure 6 represents the ASD of the raw and processed signals , together with the estimated intrinsic noise level of the LOT experiment. The residual electronics noises are compatible with the reference level of the previous configuration, on the whole frequency range. This validates the simultaneous generation of identical noisy signals.

Therefore, these first analyses show a noise reduction factor of 2×10^{10} on the electronic signals at 1 mHz. On eLISA a reduction factor of 10^9 to 10^{10} is expected.

Simulation on equal delayed perturbations To perform a first test of TDI with the LOT in a realistic configuration, a white noise (amplitude 280 Hz/$\sqrt{\text{Hz}}$) was

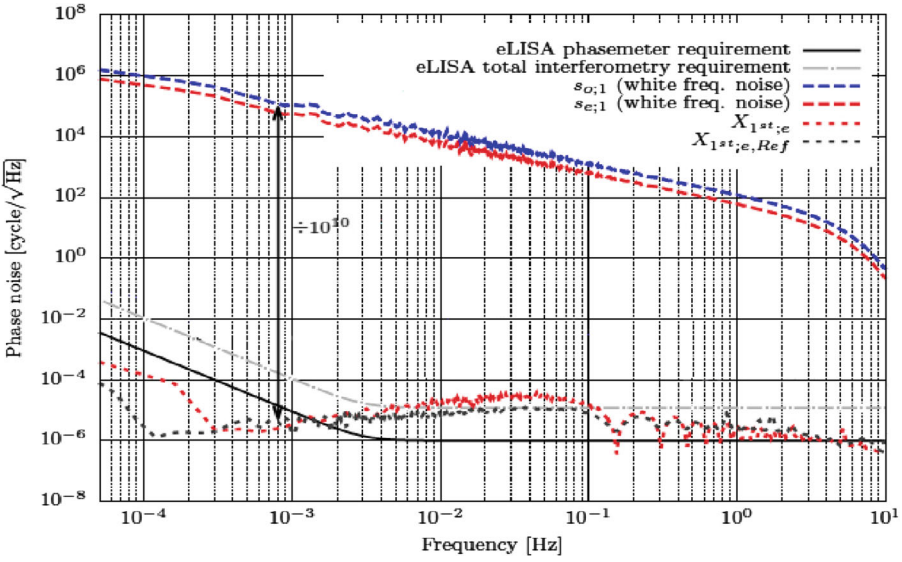

Fig. 6 Reference levels of noise in the electric LOT experiment before and after application of TDI $X_{1^{st}}$ on identical, noisy signals and comparison with the intrinsic noise level of the experiment (see Fig. 5)

simulated and applied on the local arm, as well as on the distant (delayed) arms 2 and 3 (see Fig. 7). This setup is representative of a static 'transponder' eLISA used in (4). The signal sent to the local arm is not delayed, whereas the signal on arm 2 is delayed by 6.502081 s and arm 3 by 6.502081 s (equal arm lengths configuration).

The results obtained with the equal armlengths configuration are very similar to Fig. 5. The two experiments are in fact almost identical, except for the simulation of both 'local' and 'distant' noises (therefore inducing different noise spectra of the recorded beat notes' frequencies). Consequently, the noise reduction factor for equal arm lengths, at 1 mHz, is still at the level of 2×10^{10} with the electronic interferometer.

Simulation on unequal delayed perturbations Finally, a last test is performed with the same configuration as above but with different delays on the distant arms. The signal on arm 2 is delayed by 6.502081 s and arm 3 by 6.711826 s (unequal arm lengths configuration). The resulting ASD is shown on Fig. 8.

The noise level after TDI exhibits reduced performance (by a factor of about 20), limiting the reduction factor of TDI to 5×10^8 at 1 mHz. This degradation could be due to phase jitter between the synthesized clocks driving the noise injection (1 GHz for the DDS operations) and the timestamps of the recorded phases (49.993 MHz for the phasemeter synchronization).

3.2 Description of the optical setup and optical TDI tests

The optical part of the LOT is mainly based on a Mach-Zehnder interferometer combined with AOMs (acousto-optic modulator) to shift the laser frequency on the

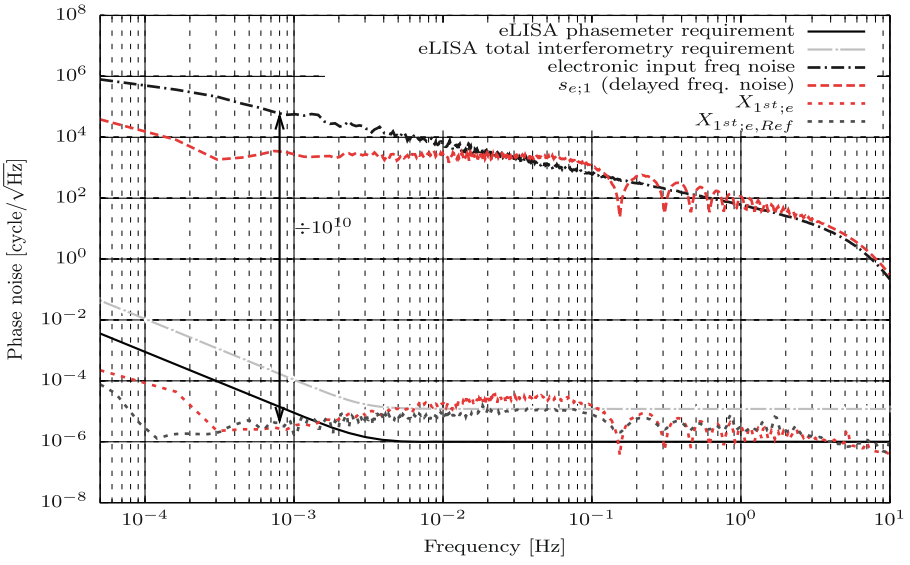

Fig. 7 Reference levels of noise in the LOT experiment before and after application of TDI $X_{1^{st}}$ on noisy signals with identical delays (6.502081 s) and comparison with the intrinsic noise level of the experiment (see Fig. 5)

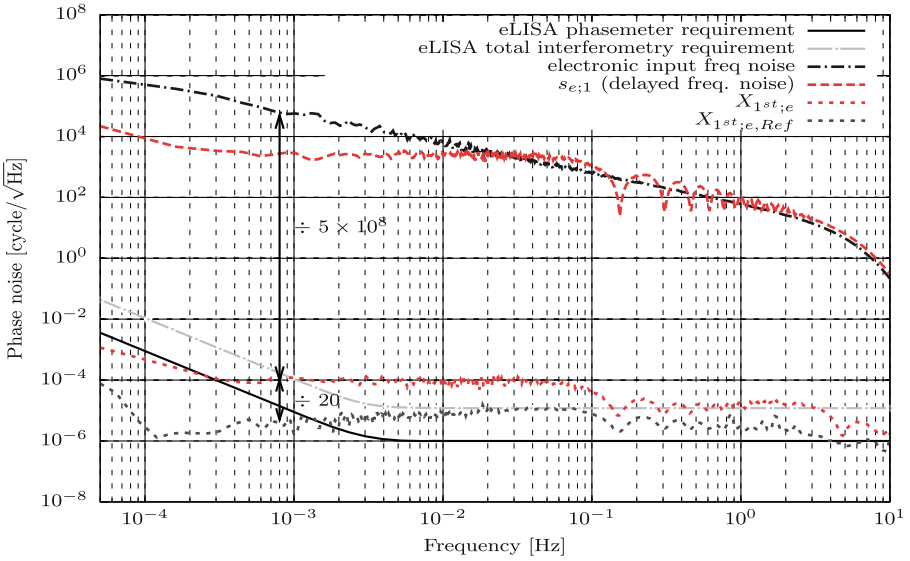

Fig. 8 Reference levels of noise in the LOT experiment before and after application of TDI $X_{1^{st}}$ on noisy signals with unidentical delays (6.502081 s and 6.711826 s) and comparison with the intrinsic noise level of the experiment (see Fig. 5)

arms in order to obtain heterodyne interferences. The beatnotes are measured by photodiodes and sent to the phasemeter.

3.2.1 General optical layout

The LOT's optical part is shown on Fig. 9. which represents one module of the simulator. The LOT is presently composed of two of those modules, each one represents one satellite of the eLISA configuration. The third module, representative of the third satellite, will be implemented in future works. For this study only one module has been used, representative of the mother S/C.

As for eLISA, the module representing one satellite has three interfering beams, one 'local' and two 'distant'. A single laser source at 1064 nm (Innolight Mephisto 500) is used to produce these beams using a combination of polarizing beam splitters (PBS) and waveplates so that optical paths of the distant beams follow the same optical path but with orthogonal polarizations.

All the experiment is performed in a clean room (ISO 8). The optical table is placed on an air cushion to reduce high frequency noise and all optical devices put under a box in order to reduce noises induced by air flow. Also, a heat device is fixed on the top to implement temperature layers so that air perturbation induced by eventual warm spots on the table are quickly absorbed.

3.2.2 Generation of the optical beat signal

The local arm's frequency can be shifted with AOM 1. In the same way, AOM 2 and 3 induce the frequency shifts for the two distant arms. Each of these distant arms

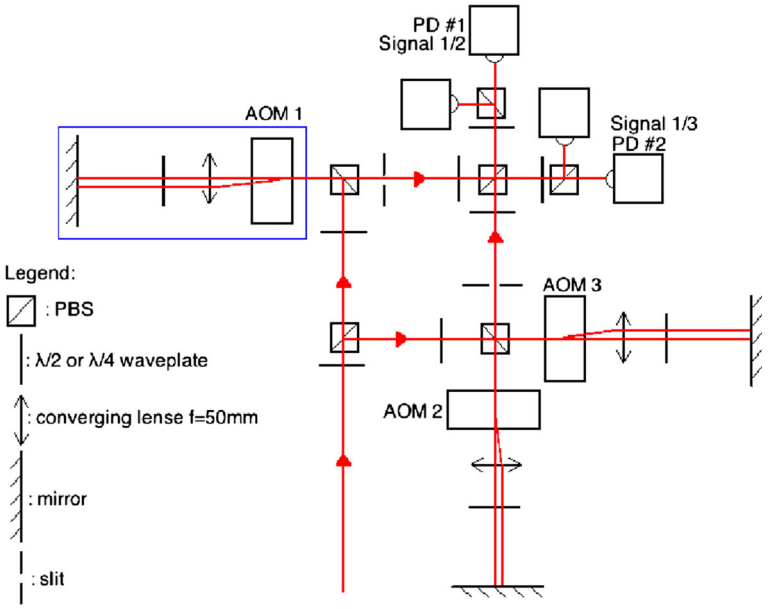

Fig. 9 Optical scheme of one module, representative of the mother S/C

interferes with the local arm to produce a heterodyne signal detected by 48 MHz bandwith photodiodes with power noise below 8 pW/$\sqrt{\text{Hz}}$. Signal 1/2 (see Fig. 10) is the resulting beatnote from the interfering beams shifted by AOM 1 and 2 and in the same way, signal 1/3 results from the interference between the beams shifted by AOM 1 and AOM 3.

Free space A&A MT110-B50 TeO2 AOMs have been used for the LOT. The maximum diffraction efficiency ($\geq$ 80 %) is reached at 110 MHz, with a bandwidth of $\pm$15 MHz with an efficiency greater than 65 %. This broad modulation bandwidth is particularly useful for simulations of the Doppler effect.

However, since a large frequency shift induces also a large angular shift after the AOM, a cat's eye configuration has been implemented for the frequency modulation represented by the blue framed part.

In such a configuration, the s-polarized laser beam is sent to the AOM using a polarizing beamsplitter (PBS). After passing through the AOM, two beams are present: the order 0 is the unaffected beam, while order 1 is frequency shifted and deflected, proportionally to the RF frequency sent to the AOM. The diffraction efficiency is also a function of the RF power.

Using a combination of lens (f = 50 mm), mirror and λ/4 waveplate, the order 1 beam is sent back on the same path with an orthogonal polarization, whatever the deflection angle (i.e. the RF frequency).When passing through the AOM, the return beam is partially frequency and angular shifted. A slit is used to only select the double shifted beam, which is then p-polarized and goes straight trough the beam splitter.

In the present experiment, RF commands around 112 and 108 MHz are sent, respectively to the two distant and to the local AOMs, producing two optical beat

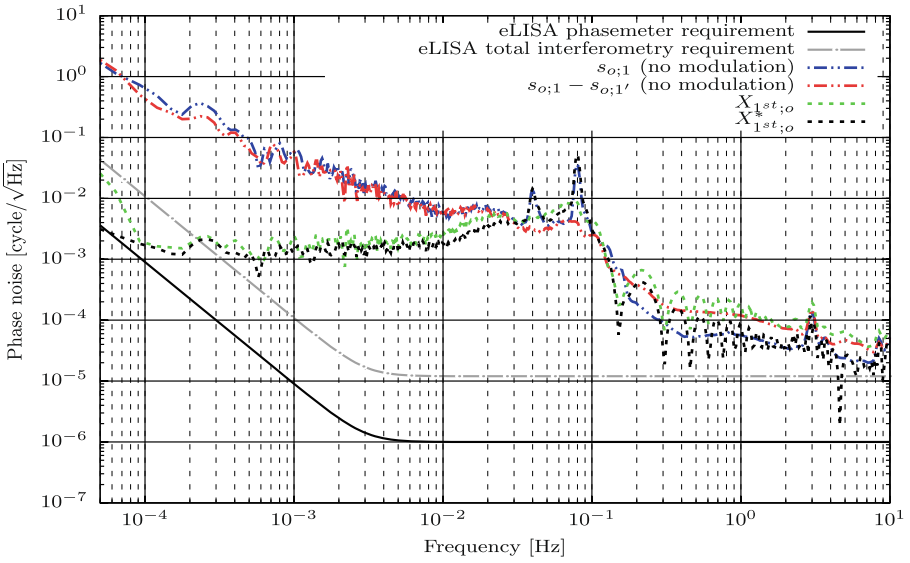

Fig. 10 Reference levels of noise in the optical LOT experiment

signals at about 8 MHz. The command frequency sent to the distant AOMs are slightly different to produce beatnotes separated by a few kHz, in order to avoid parasitic mixing from the polarization leakage of the optical components.

3.2.3 Optical TDI test

Intrinsic noise of the optical interferometer As for the electric experiment, the reference level of the optical LOT has been studied.

First we have the case where only carrier frequencies at 108.355 MHz ('local' arm), 112.572 MHz ('distant' arm 1) and 112.583 MHz ('distant' arm 2) without modulation were sent to the AOMs. The resulting beat notes are twice the value as for the electric experiment because the laser is reflected two times in the cat eye configuration. The ASD of the resulting beat note , $s_{o,1}$ and the combination $s_{o,1}$ - $s_{o,1'}$ are represented on Fig. 10.

As expected, the optical beat notes are dominated by optical pathlengths fluctuations, due to thermal expansion of the aluminium support plates, the air turbulences etc. The two optical signals are mostly uncorrelated except for the 2 resonant peaks at 0.04 and 0.08 Hz (maybe related to the air damping of the optical table).

In a second step, the 'Michelson' $X_{1^{st}}$ combination described above (5) was also tested on the optical recorded signal (with no modulation) and plotted on Fig. 10.

As for the electric experiment, this noise levels corresponds to the noise floor for the optical LOT (noted as $X_{1^{st};o,Ref}$ in the following plots).

Finally, a last test of the optical intrinsic noise was made, using again the same frequency modulation applied to the two distant AOMs (also with a white noise level of 560 Hz/$\sqrt{\text{Hz}}$ up to 1 Hz) and same delays (6.502081 s) for the two AOMs and no modulation on the local AOM. The ASD is plotted on Fig. 11.

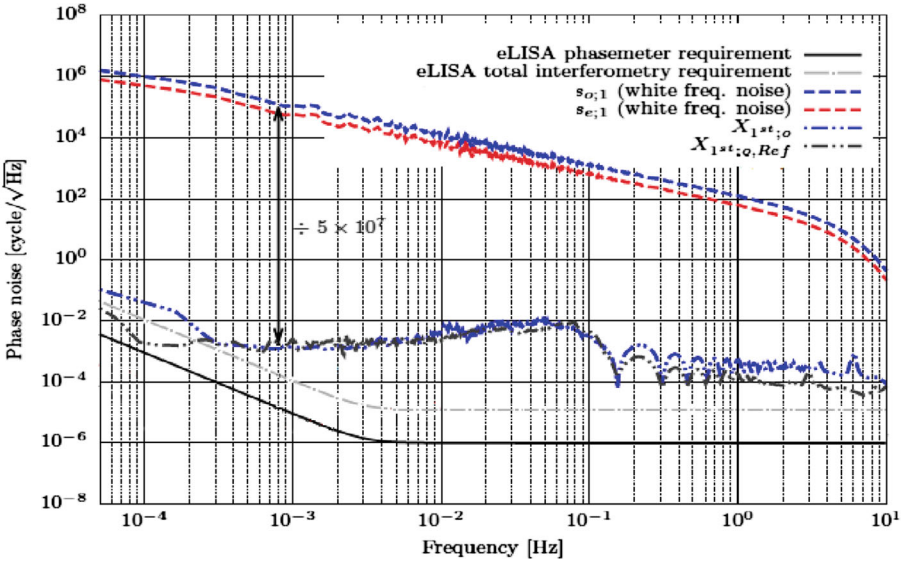

Fig. 11 Reference levels of noise in the optical LOT experiment before and after application of TDI X_{1st} on identical, noisy signals and comparison with the intrinsic noise level of the experiment (see Fig. 10)

We get a noise reduction of 5×10^7 on the optical signals at 1 mHz which is an expected decreased performance as compared to the 2×10^{10} of the electric LOT because of the optical path length fluctuations.

Simulation on equal delayed perturbations Now we show the optical results of the more realistic case of the static transponder configuration with equal arm lengths (both delays of 6.502081 s) (see Fig. 12).

The reduction level of 5×10^7 is maintained for equal arm length. This case is similar to the electric equal arm tests for which the level was also unchanged w.r.t the reference.

Simulation on unequal delayed perturbations The last measurement is the unequal arm length configuration as for the electric LOT with delays of 6.502081 s and 6.711826 s.

Figure 13 is very similar to the case of equal arm configuration. As expected, the noise level due to optical path length fluctuations hides the lower performance of the electric part for the unequal arms case.

The optical results show that the intrinsic noise level has to be lowered to be as close as possible to the electric LOT. The implementation of an optical path length compensation system has already been started and is briefly described in the next part.

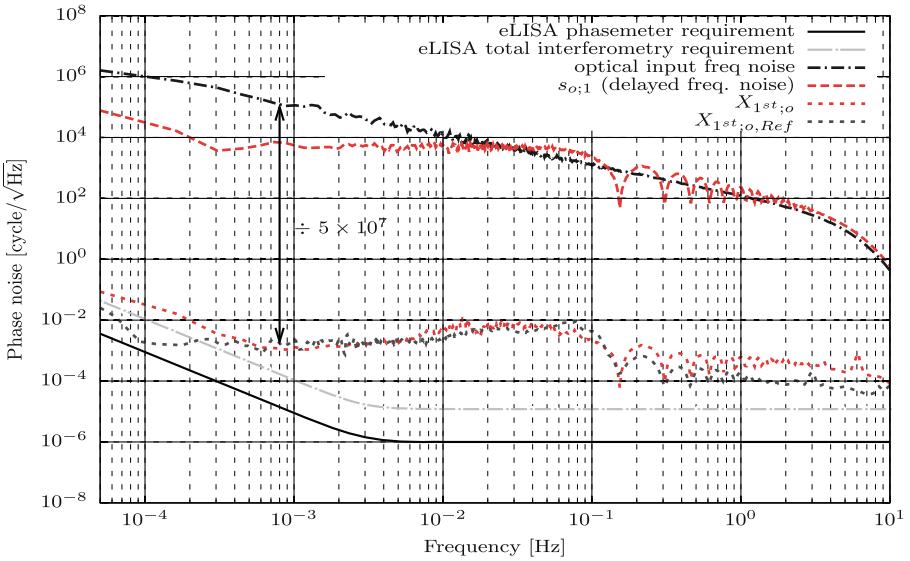

Fig. 12 Reference levels of noise in the optical LOT experiment before and after application of TDI $X_{1^{st}}$ on noisy signals with identical delays (6.502081 s) and comparison with the intrinsic noise level of the experiment (see Fig. 10)

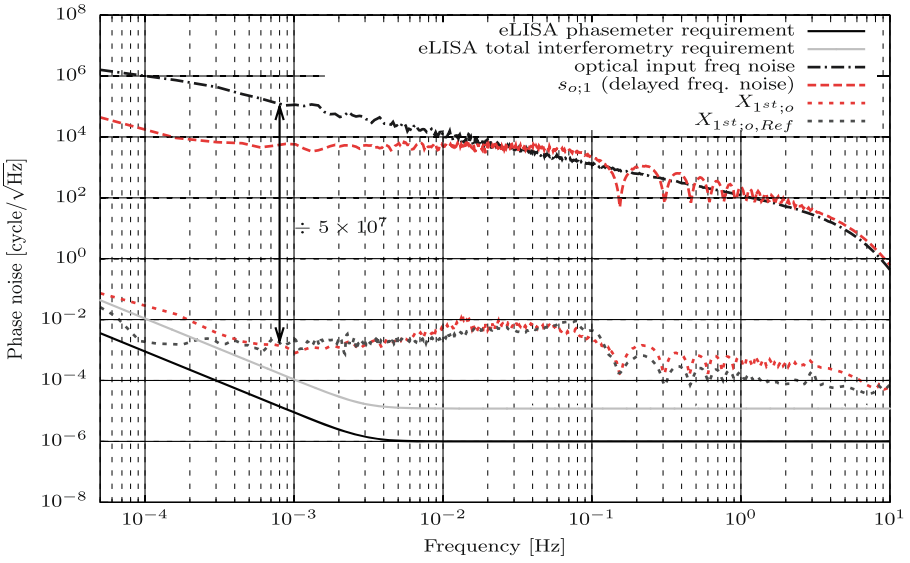

Fig. 13 Reference levels of noise in the optical LOT experiment before and after application of TDI $X_{1^{st}}$ on noisy signals with unidentical delays (6.502081 s and 6.711826 s) and comparison with the intrinsic noise level of the experiment (see Fig. 10)

4 Next steps

The results of the first measurements, as described above, demonstrate the validity of the concept but also clearly show evidence of the major sources of noise: jitter in the simulated delays and optical path-length noise. The next steps and future works will address these two points and also increase the representativity of the simulation.

First, additional measurements will be needed to clearly identify the origin of the residual noise, but some developments are already undertaken or foreseen to improve the performances of the LOT experiment.

The time jitter of the simulated delays will be addressed by inserting an FPGA (Field Programmable Gate Array) board right after the NI PXIe 6537 communication board. This FPGA will take charge of buffering, delaying and synchronizing the command frames to the AOMs. It will also allow to add frequency corrections, taken from digital or analog error signals. With the appropriate delays, this capability will mimic the phase lock of the laser sources on the distant S/C, as well as the implementation of the arm-locking stabilization scheme. This FPGA board is currently under development. Additionally, a ranging pilot tone (frequency modulation around 1 Hz) will be implemented to monitor the effective delay of the frames (this technique has already been successfully used in [16]).

The optical bench phase noise will be actively compensated using the interference of 'direct' (i.e. order 0) beams. Actually, these beams are unaffected by the RF signals on the AOMs and can be used to form an homodyne interferometer. The LOT interferometer arm lengths can therefore be stabilized using mirror dithering (above 1 kHz, i.e. outside the frequency band of eLISA) and dark fringe stabilization scheme. The homodyne and heterodyne interferometers will share almost the same optical paths (they only slightly differ between the AOMs and the end arm mirrors) and the compensation is expected to approach the interferometry requirement of eLISA.

Another effort is currently being made to couple the present command-control system for the LOT, to the LISACode simulation software [18, 19] also developed in our laboratory. Once achieved, this work will allow the simulations of realistic propagation delays, taking into account Sagnac effect, variable delays and Doppler shifts. It will also be possible to directly compare the 'numerical' results of TDI (as given by LISACode) to the same algorithm applied on optically or electronically measured beat notes.

Finally, some space has been saved on the optical bench to insert electro-optical modulators. These modulators are planned to simulate the implementation of clock noise transfer and ranging as described in [26].

5 Conclusion

We have reported the progress and first measurements of the eLISA On Table (LOT) experiment, aiming at simulating the optical beatnotes that will be recorded by long-arms space-based interferometers, such as eLISA. The principle of the experiment has been validated, with beatnotes recorded both on optical and electronics interferometers. Presently, optical bench phase noise limit the performance of the Time

Delay Interferometry (TDI) algorithm to a reduction of about 5×10^7 of the optical phase noise. Further characterization, hardware and software developments are planned to reduce the residual phase noise level and increase the similarities of the LOT with the expected implementation of eLISA.

Acknowledgments This work has been funded by the French Space Agency (CNES), under grants R-S07/SU-0001-012 and R-S08/SU-0001-012.

Appendix A: development of time delay interferometry equations

The combination of the recorded signals results in the following equations:

$$\begin{aligned} s_{TT;1} &= s_{OS;1} + \frac{s_{TO;1} + s_{Ref;1}}{2} + D_{2'1}\frac{s_{TS;2'}}{2} \\ &= D_{2'1}\eta_{L;2'} - \eta_{L;1} + g_{w;2'1} + \delta_{TM;1} + D_{2'1}\delta_{TM;2'} \\ &\quad + o_{TS;1} + D_{2'1}o_{S;2'1} \end{aligned} \tag{8a}$$

$$\begin{aligned} s_{TT;1'} &= s_{OS;1'} + \frac{s_{TO;1'} + s_{Ref;1'}}{2} + D_{31'}\frac{s_{TS;3}}{2} \\ &= D_{31'}\eta_{L;3} - \eta_{L;1'} + g_{w;31'} + \delta_{TM;1'} + D_{31'}\delta_{TM;3} \\ &\quad + o_{TS;1'} + D_{31'}o_{S;31'} \end{aligned} \tag{8b}$$

$$\begin{aligned} s_{TT;2'} &= s_{OS;2'} + \frac{s_{TO;2'}}{2} + D_{12'}\frac{s_{TS;1}}{2} \\ &= D_{12'}\eta_{L;1} - \eta_{L;2'} + g_{w;12'} + \delta_{TM;2'} + D_{12'}\delta_{TM;1} \\ &\quad + o_{TS;2'} + D_{12'}o_{S;12'} \end{aligned} \tag{8c}$$

$$\begin{aligned} s_{TT;3} &= s_{OS;3} + \frac{s_{TO;3}}{2} + D_{1'3}\frac{s_{TS;1'}}{2} \\ &= D_{1'3}\eta_{L;1'} - \eta_{L;3} + g_{w;1'3} + \delta_{TM;3} + D_{1'3}\delta_{TM;1'} \\ &\quad + o_{TS;3} + D_{1'3}o_{S;1'3} \end{aligned} \tag{8d}$$

Also, the back-link fiber being *reciprocal* [9], which means that the added noise from 1 to 1' is identical to the noise added when propagating from 1' to 1: $\eta_{B;1} = \eta_{B;1'}$,the differential noise between laser 1 and 1' can be deduced from $s_{Ref;1}$ and $s_{Ref;1'}$:

$$\frac{s_{Ref;1} - s_{Ref;1'}}{2} = \eta_{L;1} - \eta_{L;1'} + \frac{o_{Ref;1} - o_{Ref;1'}}{2} \tag{9}$$

Practically, the laser frequencies will not be let freely running but will be phase locked on a master, frequency stabilized source (e.g. Laser 1). From the previous equations, assuming perfect correction, this phase locking means that:

$$s_{Ref;1} = 0 \Rightarrow \eta_{L;1'} = \eta_{L_1} - \eta_{B;1} + o_{Ref;1} \tag{10a}$$

$$\begin{aligned} s_{OS;2'} = 0 \Rightarrow \eta_{L;2'} &= D_{12'}\eta_{L;1} + g_{w;12'} - D_{12'}\delta_{OB;1} - \delta_{OB;2'} \\ &\quad + D_{12'}o_{S;12'} + o_{OS;2'} \end{aligned} \tag{10b}$$

$$\begin{aligned} s_{OS;3} = 0 \Rightarrow \eta_{L;3} &= D_{1'3}\eta_{L;1'} + g_{w;1'3} - D_{1'3}\delta_{OB;1'} - \delta_{OB;3} \\ &\quad + D_{1'3}o_{S;1'3} + o_{OS;3} \end{aligned} \tag{10c}$$

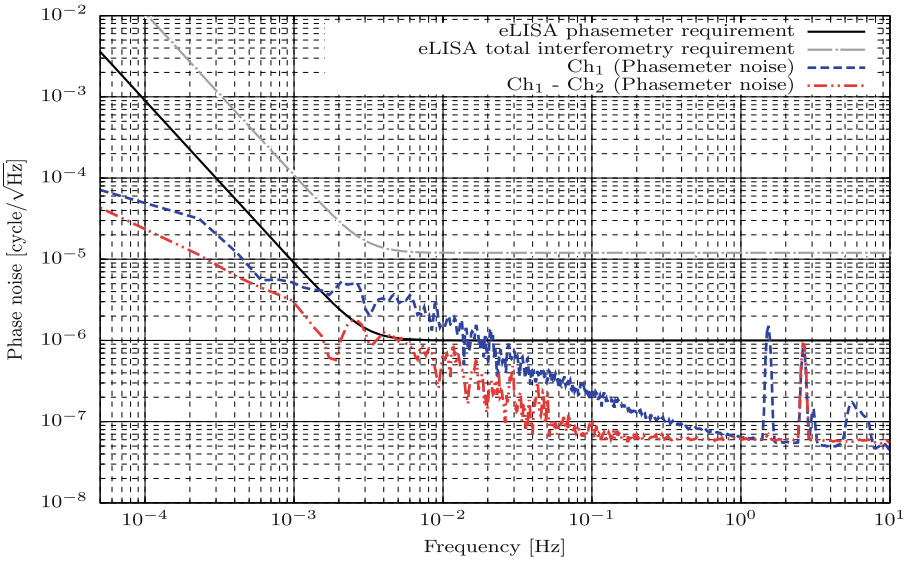

Fig. 14 Reference level of phasemeter noise

Assuming that $\delta_{OB;q} = 0$ and $\eta_{B;q} = 0$ (these noises can be subtracted using $s_{TO;q}$ and $s_{Ref;q}$ signals) and neglecting both test mass and other local noises ($\delta_{TM} = o_{xx;q} = 0$), this configuration is effectively equivalent to a transponder, where the phase noises of the incoming beams on S/C 2 and 3 are transferred on the beams sent back to S/C 1.

Appendix B: phasemeter reference measurement

The ASD of data recorded on channel 1 and the ASD of the difference between channel 1 and 2 are represented on Fig. 14.

The ASD of raw values and differences between other channels give very similar results. These results show that the raw data are slightly above the eLISA requirements for the phase measurement noise, while the differential measurement between two channels is marginally compatible with the requirement. The difference between the two curves are due to a relatively strong common mode between the channels, whose origin is unclear for the moment, but could be due, e.g. to a residual phase jitter between the reference signal (at 72.001 MHz in this experiment) and the synthesized 2.001 MHz signal.

References

1. Bykov, I., Delgado, J.J.E., Marin, A.F.G., Heinzel, G., Danzmann, K.: Lisa phasemeter development: Advanced prototyping. J. Phys. Conf. Ser. **154**(1), 012,017 (2009). http://stacks.iop.org/1742-6596/154/i=1/a=012017

2. Danzman, K. et al.: eLISA L2 White paper : The Gravitational Universe. https://www.elisascience.org/articles/elisa-mission/elisa-l2-white-paper (2013). [Online; accessed 28-August-2013]
3. Danzman, K. et al.: Elisa science web site. https://www.elisascience.org (2013). [Online; accessed 28-August-2013]
4. Danzmann, K.: {LISA} mission overview. Adv. Space Res. **25**(6), 1129–1136 (2000). doi:10.1016/S0273-1177(99)00973-4. Fundamental Physics in Space. http://www.sciencedirect.com/science/article/pii/S0273117799009734
5. Dhurandhar, S., Ni, W.T., Wang, G.: Numerical simulation of time delay interferometry for a lisa-like mission with the simplification of having only one interferometer. Adv. Space Res. **51**(1), 198–206 (2013). doi:10.1016/j.asr.2012.09.017. http://www.sciencedirect.com/science/article/pii/S0273117712005893
6. Dhurandhar, S.V.: Time-delay interferometry and the relativistic treatment of lisa optical links. J. Phys. Conf. Ser. **154**(1), 012,047 (2009). http://stacks.iop.org/1742-6596/154/i=1/a=012047
7. Esteban, J.J., García, A.F., Barke, S., Peinado, A.M., Cervantes, F.G., Bykov, I., Heinzel, G., Danzmann, K.: Experimental demonstration of weak-light laser ranging and data communication for lisa. Opt. Express **19**(17), 15,937–15,946 (2011). doi:10.1364/OE.19.015937. http://www.opticsexpress.org/abstract.cfm?URI=oe-19-17-15937
8. Esteban, J.J.J., Bykov, I., Marín, A., Heinzel, G., Danzmann, K.: Optical ranging and data transfer development for lisa. J. Phys. Conf. Ser. **154**(1), 012,025 (2009). http://stacks.iop.org/1742-6596/154/i=1/a=012025
9. Fleddermann, R., Steier, F., Tröbs, M., Bogenstahl, J., Killow, C., Heinzel, G., Danzmann, K.: Measurement of the non-reciprocal phase noise of a polarization maintaining single-mode optical fiber. J. Phys. Conf. Ser. **154**(1), 012,022 (2009). http://stacks.iop.org/1742-6596/154/i=1/a=012022
10. Heinzel, G., Esteban, J.J.J., Barke, S., Otto, M., Wang, Y., Garcia, A.F., Danzmann, K.: Auxiliary functions of the lisa laser link: ranging, clock noise transfer and data communication. Class. Quantum Gravity **28**, 4008 (2011). http://adsabs.harvard.edu/cgi-bin/nph-data_query?bibcode=2011CQGra..28i4008H&link_type=ABSTRACT
11. Jennrich, O. et al.: LISA assessment study report (Yellow Book). http://sci.esa.int/lisa/48364-lisa-assessment-study-report-yellow-book/ (2011). [Online; accessed 28-August-2013]
12. Jennrich, O. et al.: NGO assessment study report (Yellow Book). http://sci.esa.int/ngo/49839-ngo-assessment-study-report-yellow-book/ (2012). [Online; accessed 28-August-2013]
13. José Esteban, J., García, A.F., Eichholz, J., Peinado, A.M., Bykov, I., Heinzel, G., Danzmann, K.: Ranging and phase measurement for LISA. J. Phys. Conf. Ser. **228**(1), 012045 (2010). doi:10.1088/1742-6596/228/1/012045
14. McKenzie, K., Spero, R.E., Shaddock, D.A.: Performance of arm locking in lisa. Phys. Rev. D **80**, 102,003 (2009). doi:10.1103/PhysRevD.80.102003
15. Mitryk, S., Wand, V., Mueller, G.: Verification of time-delay interferometry techniques using the university of florida lisa interferometry simulator. Class. Quantum Gravity **27**, 084,012 (2010). http://www.google.com/search?client=safari&rls=en-us&q=Verification+of+time-delay+interferometry+techniques+using+the+University+of+Florida+LISA+interferometry+simulator&ie=UTF-8&oe=UTF-8
16. Mitryk, S.J., Mueller, G., Sanjuan, J.: Hardware-based demonstration of time-delay interferometry and tdi-ranging with spacecraft motion effects. Phys. Rev. D **86**, 122,006 (2012). doi:10.1103/PhysRevD.86.122006
17. Otto, M., Heinzel, G., Danzmann, K.: Tdi and clock noise removal for the split interferometry configuration of lisa. Classical and Quantum Gravity **29**(20), 205,003 (2012). http://stacks.iop.org/0264-9381/29/i=20/a=205003
18. Petiteau, A.: De la simulation de lisa a l'analyse des donnees. Ph.D. thesis, Université Paris Diderot - Paris 7 (2008)
19. Petiteau, A., Auger, G., Halloin, H., Jeannin, O., Plagnol, E., Pireaux, S., Regimbau, T., Vinet, J.Y.: Lisacode: A scientific simulator of lisa. Phys. Rev. D **77**, 23,002 (2008). doi:10.1103/PhysRevD.77.023002. http://adsabs.harvard.edu/cgi-bin/nph-data_query?bibcode=2008PhRvD..77b3002P&link_type=ABSTRACT
20. Shaddock, D.A., Tinto, M., Estabrook, F.B., Armstrong, J.W.: Data combinations accounting for lisa spacecraft motion. Phys. Rev. D **68**, 061,303 (2003). doi:10.1103/PhysRevD.68.061303
21. Shaddock, D.A., Ware, B., Spero, R.E., Vallisneri, M.: Postprocessed time-delay interferometry for lisa. Phys. Rev. D **70**, 081,101 (2004). doi:10.1103/PhysRevD.70.081101

22. Sheard, B.S., Gray, M.B., McClelland, D.E., Shaddock, D.A.: Laser frequency stabilization by locking to a {LISA} arm. Phys. Lett. A **320**(1), 9–21 (2003). doi:10.1016/j.physleta.2003.10.076. http://www.sciencedirect.com/science/article/pii/S0375960103016578
23. Sutton, A., McKenzie, K., Ware, B., Shaddock, D.A.: Laser ranging and communications for lisa. Opt. Express **18**(20), 20,759–20,773 (2010). doi:10.1364/OE.18.020759. http://www.opticsexpress.org/abstract.cfm?URI=oe-18-20-20759
24. Sutton, A., Shaddock, D.A.: Laser frequency stabilization by dual arm locking for lisa. Phys. Rev. D **78**(082), 001 (2008). doi:10.1103/PhysRevD.78.082001
25. Sutton, A.J., McKenzie, K., Ware, B., de Vine, G., Spero, R.E., Klipstein, W., Shaddock, D.A.: Improved optical ranging for space based gravitational wave detection. Class. Quantum Gravity **30**(7), 075,008 (2013). http://stacks.iop.org/0264-9381/30/i=7/a=075008
26. Sweeney, D., Mueller, G.: Experimental verification of clock noise transfer and components for space based gravitational wave detectors. Opt. Express **20**(23), 25,603–25,612 (2012). doi:10.1364/OE.20.025603. http://www.opticsexpress.org/abstract.cfm?URI=oe-20-23-25603
27. Sylvestre, J.: Simulations of laser locking to a lisa arm. Phys. Rev. D **70**, 102,002 (2004). doi:10.1103/PhysRevD.70.102002
28. Thorpe, J., Maghami, P., Livas, J.: Time domain simulations of arm locking in lisa. Phys. Rev. D **83**(12), 122,002 (2011). doi:10.1103/PhysRevD.83.122002. http://prd.aps.org/abstract/PRD/v83/i12/e122002
29. Thorpe, J.I.: Lisa long-arm interferometry. Class. Quantum Gravity **27**(8), 084,008 (2010). http://stacks.iop.org/0264-9381/27/i=8/a=084008
30. Tinto, M., Dhurandhar, S.V.: Time-delay interferometry. Living Rev. Relativ. **8**(4) (2005). doi:10.12942/lrr-2005-4. http://www.livingreviews.org/lrr-2005-4
31. Tinto, M., Shaddock, D.A., Sylvestre, J., Armstrong, J.W.: Implementation of time-delay interferometry for lisa. Phys. Rev. D **67**, 122,003 (2003). doi:10.1103/PhysRevD.67.122003
32. Tröbs, M., Heinzel, G.: Improved spectrum estimation from digitized time series on a logarithmic frequency axis. Measurement **39**(2), 120–129 (2006). doi:10.1016/j.measurement.2005.10.010
33. Tröbs, M., Heinzel, G.: Corrigendum to 'improved spectrum estimation from digitized time series on a logarithmic frequency axis' [measurement 39 (2006) 120 - 129]. Measurement **42**(1), 170 (2009). doi:10.1016/j.measurement.2008.04.004. http://www.sciencedirect.com/science/article/pii/S0263224108000705
34. Vallisneri, M.: Geometric time delay interferometry. Phys. Rev. D **72**(4), 042,003 (2005). http://scholar.google.com.rproxy.sc.univ-paris-diderot.fr/scholar?hl=en&lr=&q=info:dAzoZjt071MJ:scholar.google.com/&output=search
35. Vallisneri, M. Phys. Rev. D **76**(10), 109,903 (2007). http://scholar.google.com.rproxy.sc.univ-paris-diderot.fr/scholar?hl=en&lr=&q=info:JkBcMQqodxQJ:scholar.google.com/&output=search
36. de Vine, G., Ware, B., McKenzie, K., Spero, R.E., Klipstein, W.M., Shaddock, D.A.: Experimental demonstration of time-delay interferometry for the laser interferometer space antenna. Phys. Rev. Lett. **104**, 211,103 (2010). doi:10.1103/PhysRevLett.104.211103
37. Wand, V., Yu, Y., Mitryk, S., Sweeney, D., Preston, A., Tanner, D., Mueller, G., Thorpe, J.I., Livas, J.: Implementation of armlocking with a delay of 1 second in the presence of doppler shifts. Journal of Physics: Conference Series **154**(1), 012,024 (2009). http://stacks.iop.org/1742-6596/154/i=1/a=012024